

COUNTING DENSE OBJECTS IN REMOTE SENSING IMAGES

Guangshuai Gao[†], Qingjie Liu^{†,‡,*}, Yunhong Wang^{†,‡}

[†] The State Key Laboratory of Virtual Reality Technology and Systems, Beihang University

[‡] Hangzhou Innovation Institute, Beihang University, Hangzhou China

ABSTRACT

Estimating accurate number of interested objects from a given image is a challenging yet important task. Significant efforts have been made to address this problem and achieve great progress, yet counting number of ground objects from remote sensing images is barely studied. In this paper, we are interested in counting dense objects from remote sensing images. Compared with object counting in natural scene, this task is challenging in following factors: large scale variation, complex cluttered background and orientation arbitrariness. More importantly, the scarcity of data severely limits the development of research in this field. To address these issues, we first construct a large-scale object counting dataset based on remote sensing images, which contains four kinds of objects: buildings, crowded ships in harbor, large-vehicles and small-vehicles in parking lot. We then benchmark the dataset by designing a novel neural network which can generate density map of an input image. The proposed network consists of three parts namely convolution block attention module (CBAM), scale pyramid module (SPM) and deformable convolution module (DCM). Experiments on the proposed dataset and comparisons with state of the art methods demonstrate the challenging of the proposed dataset, and superiority and effectiveness of our method.

Index Terms— Object counting, remote sensing, attention mechanism, scale pyramid module, deformable convolution.

1. INTRODUCTION

Over the past few decades, an increasing number of researches have considered the problem of estimating the number of objects from a complex scene. As a consequence, many literatures have been published to propose models counting interested objects in images or videos across wide variety of domains such as crowding counting [1, 2, 3, 4], cell microscopy [5, 6, 7], counting animals for ecologic studies [8], vehicle counting [9, 10, 11] and environment survey [12, 13].

Albeit great progress has been made in object counting field, only a few of them have paid attention on counting objects from remotely sensed scenes, such as counting palm

and olive tress using remote sensing images [14, 15, 16] and counting vehicles based on drones [17, 18, 19]. However, the dominant ground objects in remote sensing images such as buildings, ships are ignored by the community, estimating the number of which could be beneficial for many practical applications, for instance urban planning [20], environment control and mapping [21], digital urban model construction [22] and emergency response and disaster estimation. Thus, it is of great significant to develop methods aiming to estimate number of interested objects in remote sensing images.

Compared with the counting task in other fields, counting objects in remote sensing images have the following challenges: 1) **Dataset scarcity.** The dataset for counting task is scarce in remote sensing community. Although there are datasets built for detecting or extracting objects from remote sensing images such as SpaceNet¹, DOTA² [23], these datasets are not directly suitable for counting problem, because most of images in these datasets only contain a small number of object instances, which is not enough to support the counting task; 2) **Scale variation.** Objects (such as buildings) in remote sensing images have diverse scales ranging from only a few pixels to thousands of pixels; 3) **Complex cluttered background.** Remote sensing images usually cover large scale ground areas, the objects in which coexist with complex cluttered background making them difficult to be detected, especially when they are very small; 4) **Orientation arbitrariness.** Unlike counting problem in natural images such as crowd counting under surveillance scenario, in which people walk in up-right, objects in remote sensing images have arbitrary orientations.

To remedy the aforementioned issues, we prepare to begin with two routes, one is data set, and the other is methodology. Regarding to the data set, we construct a large scale dataset for object counting task in remote sensing images. To our best knowledge, this is the first dataset built for object counting in remote sensing images. This dataset is quite large, it consists of 3057 images in total (see Table 1 for details). We hope the dataset will facilitate the research in this field. From the methodology perspective, we attempt to devise a novel neural network to address the counting problem in remote sensing images by combining attention mechanism and deformable

* Corresponding author (qingjie.liu@buaa.edu.cn).

¹<https://aws.amazon.com/public-datasets/spacenet/>

²<https://captain-whu.github.io/DOTA>

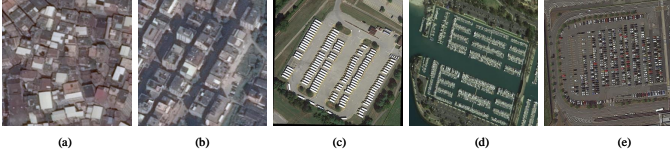


Fig. 1: Representative images of RSOC dataset. (a)-(e) represent the images of building_A, building_B, large-vehicle, ship and small-vehicle, respectively.

convolution into a unified framework, meanwhile we consider the multi-scale challenge and solved it with a scale pyramid module (SPM) [24].

The main contributions of this paper are summarized as follows:

1. We construct a large-scale remote sensing object counting dataset (RSOC) to motivate the research of object counting in remote sensing field. There are four different kinds of objects in the dataset, including buildings, ships, large vehicles and small vehicles. To the best of our knowledge, our RSOC is the first dataset ever published to study the challenging task of object counting in remote sensing images. Figure 1 shows some representative samples of our dataset.
2. We present a deep network to benchmark the object counting task in remote sensing images. The network is comprised of three modules: feature extraction with an attention module, scale pyramid module and deformable convolution module, abbreviated as ASPDNet, to address the problems of complex cluttered background, scale variation and orientational arbitrariness in remote sensing images.
3. Extensive experiments on the RSOC dataset demonstrate the effectiveness and superiority of our proposed framework, which significantly outperforms the baseline methods.

Table 1: There are four different kinds of objects in the dataset: building, ship, large vehicle and small vehicle. We split the dataset into five subsets according to the density levels of the objects. Building_A has larger density level than Building_B. It also worth noting that for data annotation, building subsets are labeled with center point, and other three ones adopt bounding box, preprocessing to compute their center points when generating their ground truth density maps.

Dataset	Images	Training/Test	Average Resolution	Statistics			
				Total	Min	Average	Max
Building_A	360	179/181	512 × 512	19,963	34	55.45	142
Building_B	2108	1026/1082	512 × 512	56,252	15	26.69	76
Ship	137	97/40	2558 × 2668	44,892	50	327.68	1661
Large-vehicle	172	108/64	1552 × 1573	16,594	12	96.48	1336
Small-vehicle	280	222/58	2473 × 2339	148,838	17	531.56	8531

2. METHODOLOGY

2.1. Overview

The architecture of the proposed network is illustrated in Figure 2. The ASPDNet is comprised of three parts: the front-end is a truncated VGG16 [25] (the last two pooling layers and fully-connected layers are removed), followed by an attention module [26]; the mid-end is a scale pyramid module (SPM) [24] consisting of four dilated convolution layers with different dilation rates, and followed by several regular convolution layers; the back-end is a set of deformable convolution layers [27]. And finally one 1×1 convolution layer is executed to obtain the predicted density map. The final count can be computed by summing all the pixel values of the density map. The detailed introduction of each component in our proposed ASPDNet will be elaborated in the following subsections.

2.1.1. Feature extraction with attention module (front-end)

Given a remote sensing image with arbitrary size, we first feed it into a feature extractor, which is composed of the first 10 convolution layers of VGG16 [25] with all filters have 3×3 kernel sizes. After that, we add an attention module to capture more contextual and high-level semantic information, which is helpful to suppress the cluttered backgrounds meanwhile highlight the object regions. We draw inspiration from the CBAM network [26] and design an lightweight attention module which consists of a sequential of channel-spatial attention operation. The structure of this attention module is shown in Figure 2.

2.1.2. Scale pyramid module (mid-end)

Since there are three max-pooling operations in the front-end stage, the size of the output feature maps are $1/64$ of the original input size. To enlarge the receptive field while retaining the resolution of the feature maps, a scale pyramid module (SPM) [24] is introduced, which concatenates several dilated convolutions with different dilated rates. Empirically, we set the number of dilated convolutions [28] as 4 and the dilated rates as 2, 4, 8, 12, as adopted in [24]. With the SPM, multi-scale features and finer information are captured to enhance the robustness of the model to scale variation.

2.1.3. Deformable convolution module (back-end)

Deformable convolution [27] is an operation which adds an offset, whose magnitude is learnable, on each point in the receptive field of feature map. After the offset, the shape of receptive field is matching the actual shape of the object rather than a square. The advantage of the offset is that no matter how deformable the object is, the region of convolution always can cover the object. Benefiting from the adaptive

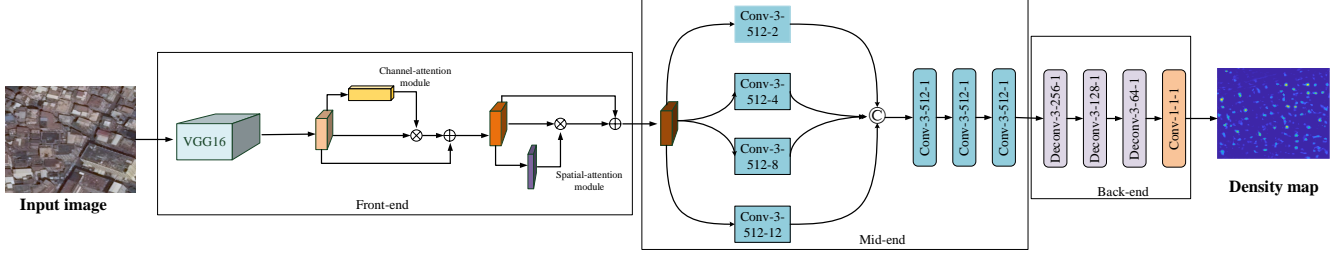


Fig. 2: Architecture of ASPDNet. The parameters of convolutional layers in the mid-end stage are denoted as “Conv-(kernel size)-(number of filters)-(dilation rate)”, while the parameters in the back-end stage are represented as “Deconv-(kernel size)-(number of filters)-(stride)”. The max-pooling layers are conducted over a 2×2 pixel window, with stride 2 (ignored in the figure). “ \oplus ”, “ \otimes ” and “ \odot ” represent matrix addition, matrix multiplication and matrix concatenation operation, respectively.

sampling location mechanism in the deformable convolution module (DCM), the offset can be adjusted and optimized via training. Rather than uniform sampling, the dynamic sampling scheme can be better suited to cope with the orientation arbitrariness due to overhead perspective in the remote sensing images.

2.2. Ground truth density maps generation

We use density map as ground truth to optimize and test the models. Following the procedure of density map generation in [1], one object instance at pixel x_i ³ can be represented by a delta function $\delta(x - x_i)$. Therefore, given an image with N instances annotated, its ground truth can be represented as follows:

$$H(x) = \sum_{i=1}^N \delta(x - x_i) \quad (1)$$

To generate the density map F , we convolute $H(x)$ with a Gaussian kernel, which can be defined as follows:

$$F(x) = \sum_{i=1}^N \delta(x - x_i) * G_{\sigma_i}(x) \quad (2)$$

where σ_i represents the standard deviation, empirically, we adopt the fixed kernel with $\sigma = 15$ for all the experiments.

2.3. Training details

The proposed method is trained in an end-to-end manner. The first 10 convolutional layers are fine-tuned from VGG16 [25], and the other layers are initialized through a Gaussian initialization with a 0.01 standard deviation. During training, stochastic gradient descent (SGD) is applied, and learning rate is set as $1e-5$. We adopt the batch size of 32 for the Building datasets, 1 for the other three sub-datasets. The trainings take 400 epochs to convergence.

Following previous works [1, 29, 30], we employ the Euclidean distance as loss function to train the network.

³Here x_i is the center of the object.

3. EXPERIMENTS

In this section, we evaluate the proposed counting method on our RSOC dataset, which is divided into five subsets: Building_A, Building_B, Ship, Large vehicle and Small vehicle. We report results of the proposed and comparison methods on these five subsets. The implementation of our models are based on Pytorch framework [31].

3.1. Evaluation metrics

For object counting in remote sensing images, two metrics are adopted to measure the performance of proposed approach: Mean Absolute Error (MAE) and Root Mean Squared Error (RMSE), of which MAE measures the accuracy of the method, while RMSE measures the robustness. These two metrics are defined as:

$$MAE = \frac{1}{N} \sum_{i=1}^N |C_i^{pred} - C_i^{GT}| \quad (3)$$

$$RMSE = \sqrt{\frac{1}{N} \sum_{i=1}^N |C_i^{pred} - C_i^{GT}|^2} \quad (4)$$

where N is the number of test images, C_i^{pred} denotes the predicted counting for i -th image and C_i^{GT} indicates the ground-truth.

3.2. Data augmentation

To better train the proposed approach, we augment the training set as follows: for each training image, 9 sub-images with 1/4 size of the original image are cropped. Of which, four patches are non-overlapping sub-images. While other five patches are cropped from the input image randomly. Then, we double the generated training by applying horizontal flipping of crops. For Large-vehicle, Small-vehicle and Ship subsets which are with large image sizes, we resize all images into a fixed image size of 1024×768 before data augmentation.

Table 2: Performance comparison on Building_A and Building_B dataset.

Method	Building_A		Building_B	
	MAE	RMSE	MAE	RMSE
MCNN [1]	14.33	19.47	13.11	16.60
CMTL [3]	15.04	20.77	10.24	13.64
CSRNet [2]	13.32	18.00	7.37	10.32
SFCN [4]	13.14	17.56	6.31	8.33
ASPDNet(our proposed)	10.21	14.27	5.31	7.02

Table 3: Performance comparison on Ship-, Large-vehicle and Small-vehicle sub datasets.

Method	Ship		Large-vehicle		Small-vehicle	
	MAE	RMSE	MAE	RMSE	MAE	RMSE
MCNN [1]	263.91	412.30	36.56	55.55	488.65	1317.44
CMTL [3]	251.17	403.07	61.02	78.25	490.53	1321.11
CSRNet [2]	240.01	394.16	34.10	46.42	443.72	1252.22
SFCN [4]	240.16	394.81	33.93	49.74	440.70	1248.27
ASPDNet(our proposed)	193.83	318.95	31.76	40.14	433.23	1238.61

3.3. Comparison with state-of-the-arts

We compare our method with four state of the art models, including MCNN [1], CMTL [3], CSRNet [2] and SFCN [4]. These four methods are proposed to address crowd counting issue, however they are applicable for other counting problems. We fine-tune them on the training set of our dataset and report the results on the testing set. Table 2 and Table 3 list the quantitative metrics of the proposed and comparison methods on the subsets of the proposed dataset. Table 2 depicts that our proposed method outperforms other methods by a large margin both on Building_A and Building_B. Table 3 reveals that our proposed method can achieve marginally better results than the comparisons even on the challenging Ship and Small-vehicle sets. There is still much room to be improved on these two subsets, indicating the challenging nature of the proposed dataset.

Some visual results, i.e. the predicted density maps and the estimated number of objects are shown in Figure 3. The top row are input images, the middle row are ground-truth density maps, and the bottom are the density maps generated by proposed method. The ground truth count and predicted count are located at the left-bottom corner of the density maps. It can be observed from Figure 3, our estimated counts are very close to the ground truths.

3.4. Ablation study

To validate the effect of each module (CBAM, SPM and DCM), some ablation experiments are conducted on the Building dataset. Table 4 demonstrates the performance of models with different settings. The baseline of this paper is CSRNet [2], and the three modules are successively added on the top of the baseline.

From the Table 4, we can see that each component in our network contributes to the performance improvement to some extent. As a consequence, our proposed ASPDNet, which incorporates CBAM, SPM and deformable convolution into a

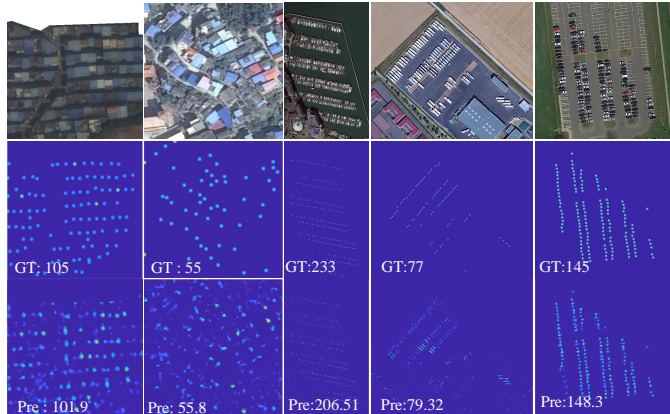


Fig. 3: Predicted results of our proposed method. The top row are input images, the middle row are ground truth density maps and the bottom row are our predicted density maps. From the left to right, the images are from the five sub-set of our constructed dataset.

Table 4: Ablation studies on Building_A and Building_B dataset.

Method	Building_A		Building_B	
	MAE	RMSE	MAE	RMSE
Baseline	13.32	18.00	7.37	10.32
Baseline+CBAM	12.95	17.51	7.71	9.90
Baseline+CBAM+SPM	12.28	16.52	5.67	7.28
ASPDNet	10.21	14.27	5.31	7.02

unified framework, improves the performance by a large margin compared with the baseline model. To be specific, our proposed ASPDNet reduces by **23.35%** / **20.72%** and **27.95%** / **31.98%** in terms of MAE / RMSE on the Building_A and Building_B dataset, respectively.

4. CONCLUSION

In this paper, we have presented a single column deep network named as ASPDNet for object counting in remote sensing images. The network incorporates attention module, scale pyramid module and deformable convolution module into a unified framework. To benchmark our proposed method, a new large-scale object counting dataset (RSOC) is constructed. Extensive experimental results demonstrate that the effectiveness and superiority of our proposed approach. We expect that our contribution can bridge the gap and promote the new developments on the object counting in the remote sensing field.

Acknowledgement

This work was supported by the National Natural Science Foundation of China (Grant Nos: 41871283, U1804157 and 61601011).

5. REFERENCES

- [1] Yingying Zhang, Desen Zhou, Siqin Chen, Shenghua Gao, and Yi Ma, “Single-image crowd counting via multi-column convolutional neural network,” in *CVPR*, 2016, pp. 589–597. 1, 3, 4
- [2] Yuhong Li, Xiaofan Zhang, and Deming Chen, “Csrnet: Dilated convolutional neural networks for understanding the highly congested scenes,” in *CVPR*, 2018, pp. 1091–1100. 1, 4
- [3] Vishwanath A Sindagi and Vishal M Patel, “Cnn-based cascaded multi-task learning of high-level prior and density estimation for crowd counting,” in *AVSS*. IEEE, 2017, pp. 1–6. 1, 4
- [4] Qi Wang, Junyu Gao, Wei Lin, and Yuan Yuan, “Learning from synthetic data for crowd counting in the wild,” in *CVPR*, 2019, pp. 8198–8207. 1, 4
- [5] Yi Wang and Yuexian Zou, “Fast visual object counting via example-based density estimation,” in *ICIP*. IEEE, 2016, pp. 3653–3657. 1
- [6] Elad Walach and Lior Wolf, “Learning to count with cnn boosting,” in *ECCV*. Springer, 2016, pp. 660–676. 1
- [7] Victor Lempitsky and Andrew Zisserman, “Learning to count objects in images,” in *NIPS*, 2010, pp. 1324–1332. 1
- [8] Carlos Arteta, Victor Lempitsky, and Andrew Zisserman, “Counting in the wild,” in *ECCV*. Springer, 2016, pp. 483–498. 1
- [9] Daniel Onoro-Rubio and Roberto J López-Sastre, “Towards perspective-free object counting with deep learning,” in *ECCV*. Springer, 2016, pp. 615–629. 1
- [10] Hanwang Zhang, Zawlin Kyaw, Shih-Fu Chang, and Tat-Seng Chua, “Visual translation embedding network for visual relation detection,” in *CVPR*, 2017, pp. 5532–5540. 1
- [11] Shanghang Zhang, Guanhang Wu, Joao P Costeira, and José MF Moura, “Fcn-rlstm: Deep spatio-temporal neural networks for vehicle counting in city cameras,” in *ICCV*, 2017, pp. 3667–3676. 1
- [12] Geoffrey French, MH Fisher, Michal Mackiewicz, and CL Needle, “Convolutional neural networks for counting fish in fisheries surveillance video,” *MVAB*, pp. 1–7, 2015. 1
- [13] Beibei Zhan, Dorothy N Monekosso, Paolo Remagnino, Sergio A Velastin, and Li-Qun Xu, “Crowd analysis: a survey,” *MVA*, vol. 19, no. 5-6, pp. 345–357, 2008. 1
- [14] Esther Salami, Antonia Gallardo, Georgy Skorobogatov, and Cristina Barrado, “On-the-fly olive trees counting using a uas and cloud services,” *Remote Sensing*, vol. 11, no. 3, pp. 316, 2019. 1
- [15] Nurulain Abd Mubin, Eiswary Nadarajoo, Helmi Zulhaidi Mohd Shafri, and Alireza Hamedianfar, “Young and mature oil palm tree detection and counting using convolutional neural network deep learning method,” *IJRS*, vol. 40, no. 19, pp. 7500–7515, 2019. 1
- [16] Yakoub Bazi, H Al-Sharari, and Farid Melgani, “An automatic method for counting olive trees in very high spatial remote sensing images,” in *IJRSS*. IEEE, 2009, vol. 2, pp. 125–128. 1
- [17] T Nathan Mundhenk, Goran Konjevod, Wesam A Sakla, and Kofi Boakye, “A large contextual dataset for classification, detection and counting of cars with deep learning,” in *ECCV*. Springer, 2016, pp. 785–800. 1
- [18] Meng-Ru Hsieh, Yen-Liang Lin, and Winston H Hsu, “Drone-based object counting by spatially regularized regional proposal network,” in *ICCV*, 2017, pp. 4145–4153. 1
- [19] Yuanqiang Cai, Dawei Du, Libo Zhang, Longyin Wen, Weiqiang Wang, Yanjun Wu, and Siwei Lyu, “Guided attention network for object detection and counting on drones,” *arXiv preprint arXiv:1909.11307*, 2019. 1
- [20] M Mazhar Rathore, Awais Ahmad, Anand Paul, and Seungmin Rho, “Urban planning and building smart cities based on the internet of things using big data analytics,” *Computer Networks*, vol. 101, pp. 63–80, 2016. 1
- [21] Jean-François Pekel, Andrew Cottam, Noel Gorelick, and Alan S Belward, “High-resolution mapping of global surface water and its long-term changes,” *Nature*, vol. 540, no. 7633, pp. 418, 2016. 1
- [22] Li Guan, Yanjie Ding, Xuebing Feng, and Hui Zhang, “Digital beijing construction and application based on the urban three-dimensional modelling and remote sensing monitoring technology,” in *IGARSS*. IEEE, 2016, pp. 7299–7302. 1
- [23] Gui-Song Xia, Xiang Bai, Jian Ding, Zhen Zhu, Serge Belongie, Jiebo Luo, Mihai Datcu, Marcello Pelillo, and Liangpei Zhang, “Dota: A large-scale dataset for object detection in aerial images,” in *CVPR*, 2018, pp. 3974–3983. 1
- [24] Xinya Chen, Yanrui Bin, Nong Sang, and Changxin Gao, “Scale pyramid network for crowd counting,” in *WACV*. IEEE, 2019, pp. 1941–1950. 2
- [25] Karen Simonyan and Andrew Zisserman, “Very deep convolutional networks for large-scale image recognition,” *arXiv preprint arXiv:1409.1556*, 2014. 2, 3
- [26] Sanghyun Woo, Jongchan Park, Joon-Young Lee, and In So Kweon, “Cbam: Convolutional block attention module,” in *ECCV*, 2018, pp. 3–19. 2
- [27] Jifeng Dai, Haozhi Qi, Yuwen Xiong, Yi Li, Guodong Zhang, Han Hu, and Yichen Wei, “Deformable convolutional networks,” in *ICCV*, 2017, pp. 764–773. 2
- [28] Fisher Yu and Vladlen Koltun, “Multi-scale context aggregation by dilated convolutions,” *ICLR*, 2015. 2
- [29] Lokesh Boominathan, Srinivas SS Kruthiventi, and R Venkatesh Babu, “Crowdnet: A deep convolutional network for dense crowd counting,” in *ACM MM*. ACM, 2016, pp. 640–644. 3
- [30] Deepak Babu Sam, Shiv Surya, and R Venkatesh Babu, “Switching convolutional neural network for crowd counting,” in *CVPR*. IEEE, 2017, pp. 4031–4039. 3
- [31] Adam Paszke, Sam Gross, Soumith Chintala, and Gregory Chanan, “Pytorch: Tensors and dynamic neural networks in python with strong gpu acceleration,” *PyTorch: Tensors and dynamic neural networks in Python with strong GPU acceleration*, vol. 6, 2017. 3